Asia-Pacific Journal of Science and Technology: Volume: 29. Issue: 01. Article ID.: APST-29-01-13. Research Article

APST

Asia-Pacific Journal of Science and Technology

https://www.tci-thaijo.org/index.php/APST/index

Published by the Research and Graduate Studies Division,
Khon Kaen University, Thailand

Detection of antibacterial activity of zinc oxide nanoparticles prepared by *Punica granatum*

Lina M. Alnaddaf [1,*], Mohamad N. Ksaier [2] and Raed A.R. Almohammad[2]

[1]Biotechnology and Molecular Biology, Department of field crops, College of Agriculture, Albaath University, Homs, Syria
[2]Medico Labs, Homs, Syria
[*]Corresponding author: lalnaddaf@albaath-univ.edu.sy

Received 26 October 2022
Revised 29 December 2022
Accepted 11 January 2023

Abstract

Nanotechnology contributes novel tools to achieve sustainable development in the health sector. Nanomaterials (NMs) interact with microorganisms with various mechanisms, leading to negative or positive effects. This contributes to reducing bacterial resistance to antibiotics and enhances human health. In this study, green synthesis of zinc oxide nanoparticles (ZnONPs) was prepared from *Punica granatum* peel extracts of pericarp (per) and membrane (m) in Biotechnology Center at Al-Baath University in 2022. Ultraviolet-visible spectroscopy (UV-Vis), Fourier transform infrared (FTIR), Scanning Electron Microscope (SEM) and X-ray diffraction (XRD) characterized the ZnONPs (per and m). Then, the well diffusion method, antibacterial activity was estimated against *Staphylococcus aureus* (ATCC-6538) and *Escherichia coli* (ATCC-8739). The synergistic effects of antibiotics clindamycin and ciprofloxacin were evaluated in combination with NPs. The results of UV-Vis showed the presence of peaks at 366 and 369 nm for ZnONPs respectively. The FTIR spectra indicated functional groups related to O-H, C-C, C=C, C=O, C-O, C-N, C-H, P-O-C, C-CL and ZnO. The morphological shape and size of ZnONPs (per and m) via SEM were 33-51 nm respectively. Low crystalline was for both ZnONPs in the X-ray spectrum. ZnONPs m showed high activity against *S. aureus*. ZnONPs per had better activity than ZnONPs m against *E. coli*. ZnONPs had a synergy effect with both antibiotics. *E. coli* are more sensitive to ciprofloxacin+ZnONPs (per and m) solutions. The biosynthesized ZnONPs offer probable applications as antibacterial agents. The combination between nanoparticles (NPs) and antibiotics formulates new prospects for future studies and enhances the synergistic effects against antibiotic-resistant bacteria.

Keywords: Biosynthesis, Secondary metabolites, Zinc oxide nanoparticle, *Punica granatum*, Antibacterial activity, synergistic effects

1. Introduction

Green synthesis is an advanced innovation that utilizes plant extract to prepare nanomaterials (NMs) that lead to a new era in synthesizing stable nanoparticles (NPs) and increases the life of NPs [1]. NPs possess various applications in different scientific and technological fields, and this leads to high demand for producing NPs [2]. There are various methods to manufacture NPs such as chemical, physical and biosynthesis. The first depends primarily on chemical reactions with their risks and side effects. While physical methods are more complicated and economically expensive [3]. To search for safe, cheap, and environmentally friendly methods for synthesizing NPs, plant secondary metabolites as manufacturing methods have been chosen. These consider agents for reducing, stabilizing, and capping NPs in the process of NM synthesis [4].

Plant extracts have various biomolecules, such as caffeine, ketones, polyphenols, ascorbic acids, proteins, flavones, enzymes, amino acids, aldehydes, carboxylic acids, polysaccharides and terpenoids, which are considered as reducing agents for metal ions. For this reason, there is diversity in NPs morphology (triangular, hexagonal, spherical, cubic and pentagon) which is related to the interaction between biomolecular and metal ions

[5]. Many studies indicated the synthesis of zinc oxide nanoparticles (ZnONPs) which had various forms, this depends on resources for the synthesis of ZnONPs such as *Punica granatum* [6].

Punica granatum fruit has superior therapeutic properties and health benefits for consumers. It contains a high number of secondary metabolites as sources of natural antioxidants [7]. Previously reported, identified some major compounds in it include granatin A and granatin B, gallic acid, punicalagin, chlorogenic acid, ellagic acid, caffeic acid, punicalin, quercetin, apigenin, cyanidin, pelargonidin. These compounds are utilized in the biosynthesis of different NPs [8].

The properties of ZnONPs make its applications include cosmetic industry [9] antibacterial activity, antifungal activity [10] and catalytic activity [11]. Presently, antibiotic resistance, a lot of mutations and new pathogenic strains are increasing. So, the priority now is detecting more effective antibacterial agents. Impact biological functions of zinc oxide depend on its concentration, particle size, exposure time, morphology, and pH [9].

ZnONPs are more effective against microorganisms such as *Staphylococcus aureus*, *Bacillus megaterium*, *Bacillus subtilis*, *Sarcina lutea*, *Escherichia coli*, *Klebsiella pneumonia*, *Pseudomonas aeruginosa*, *Pseudomonas vulgaris*, *Aspergillus niger* and *Candida albicans* [12]. ZnONPs have been effective in inhibiting the growth of microorganisms by permeating the cell membrane and accumulating ZnONPs in the cytoplasm which reacts with biomolecules leading to cell apoptosis. In addition, ZnONPs lead to oxidative stress which causes damage to vital component functions [13].

The high prevalence of multidrug-resistant bacteria demands using new strategies such as nanotechnology to overcome its resistance. Metallic NPs are considered promising agents in antibacterial due to their biological and chemical properties that make them toxic to it [14].

Recent studies indicated the importance of combining NPs with antibiotics to decrease dosages, increase their bactericidal properties and enhance the ability of antibiotics to interact with bacteria leading to real synergy against its resistance [12]. For instance, Thati et al. [15] reported that the Combination between ZnONPs and antibiotics using the disk diffusion method increased the inhibition zones against *S. aureus*. Likewise, Banoee et al. [16] studied the combined influence of ZnONPs with various antibiotics against *E. coli* and *S. aureus* via calculate the percentage of inhibition zone areas. Ciprofloxacin presented beneficial interactions with ZnONPs, it increases in inhibition zone areas by about 27 and 22% against *S. aureus* and *E. coli* respectively.

So, the aim of this research was to utilization of the secondary metabolites of pericarp and membrane of *P. granatum* as an eco-friendly, cheap method for the biosynthesis of ZnONPs and compared its antibacterial activity against both gram-positive and negative bacteria. In addition, evaluation of the synergistic effects resulting from the combination between ZnONPs and antibiotics.

2. Materials and methods

2.1 Extraction of pomegranate peels

The healthy Pomegranate (*Punica granatum* L.) fruits were utilized from safita farms in Tartous city and washed with distilled water. The pomegranate fruits were cut manually, separated pericarps (per) and membranes (m) (The membranes between seeds), collected, and dried at room temperature. Then, get the powder by using a blender and keeping it at 4°C [17].

Prepare two samples: the first from (per) and the second from (m) dry powder. Ten grams of both alone were mixed with 100 mL of deionized distilled water then the mixture was stirred for 15 min at 60-70°C. Then, the solutions were centrifuged at 4000 rpm for 10 min and repeated three times. The aqueous extractions for the per and m are kept at 4°C until use [18].

2.2 Green synthesis of ZnONPs

Green Synthesis of ZnONPs from per and m was prepared. 2.97 g of Zinc nitrate ($Zn(NO_3)_{2\cdot6}H_2O$) was added to the flask containing 100 mL of deionized distilled water under magnetic stirring at 80°C for 20 min. Then, slowly add the aqueous extract of pomegranate peels (per and m) to obtain the colored solution [17].

2.3 Characterization of ZnO NPs

The ZnONPs (per and m) were characterized by ultraviolet-visible spectroscopy (UV-Vis) spectra of 200-900 nm (T80+UV/Vis spectrometer. PG Instruments Ltd). In addition, the measurement of functional groups of powder for (per and m) and ZnONPs (per and m) was done in terms of transmittance (400 to 4000 cm^{-1} range) by the Fourier Transform Infrared spectrometer (Fourier transform infrared (FTIR)-4100). Whereas to determine the shape and size of ZnONPs (per and m) were utilized by Scanning Electron Microscope (SEM). Also, X-ray diffraction (XRD) was done to analyze the crystalline nature and the morphology of zinc oxide nanoparticles synthesized from Per and m by using radiation with Cu Kα1, ƛ= 1.5401Å at 2 theta (20º-80º) [19].

2.4 Antibacterial activity for biosynthesized ZnONPs (per and m)

Mueller Hinton Agar (MHA) medium was prepared and autoclaved at 121°C for 20 min to evaluate the antibacterial activity of the synthesized ZnONPs from both (per and m) of pomegranate against two pathogenic bacterial strains *Staphylococcus aureus* (ATCC-6538) and *Escherichia coli* (ATCC-8739). Also, bacterial suspension was utilized (1.5×10^8 colony-forming unit (CFU)/mL) and the well diffusion method was used. Herein, (10 mg) of ZnONPs were dissolved in (1 mL) deionized distilled water + (1 mL) dimethyl sulfoxide (DMSO). After that thirty-six Petri plates with MHA medium with two bacterial suspensions and two kinds of ZnONPs (per and m) were cultured. 6 wells were punched on the Petri plate, each of its, respectively, contained ZnONPs, DMSO, antibiotics (ciprofloxacin for *E. coli* and clindamycin for *S. aureus*) and (antibiotics+ZnONPs) Table 1, and incubated at 37°C for 24 h. Then inhibition zone diameter data of bacteria growth were measured in millimeters and recorded [20].

Table 1 The wells in the Petri plate.

Number	Tested material	Solvent
1	ZnONPs 10 mg	1 mL deionized distilled water+ 1 mL DMSO
2	ZnONPs 10 mg+50 mg ciprofloxacin	1 mL deionized distilled water+ 1 mL DMSO
3	50 mg ciprofloxacin	1 mL deionized distilled water
4	ZnONPs 10 mg+10 mg clindamycin	1 mL deionized distilled water+ 1 mL DMSO
5	10 mg clindamycin	1 mL deionized distilled water
6	Tested material	1 mL DMSO

2.5 Statistical analysis

Statistical analysis was conducted using a statistical package for the social science (SPSS) program. As well as calculating the value of the least significant difference (L.S.D) at the level of significance 1%, comparing the averages and determining the significance of the differences between them.

3. Results and discussion

3.1 Biosynthesis and characterization of ZnONPs

3.1.1 UV-Vis

UV-visible spectroscopy is usually performed to confirm the synthesis of ZnONPs resulting from the Surface Plasmon Resonance (SPR) effect. The peak obtained at 366 and 369 nm clearly illustrates the presence of ZnONPs (per and m) respectively in the solution. Also, we observed the same peak after two months of manufacturing. This indicated the stability of ZnONPs Figure 1.

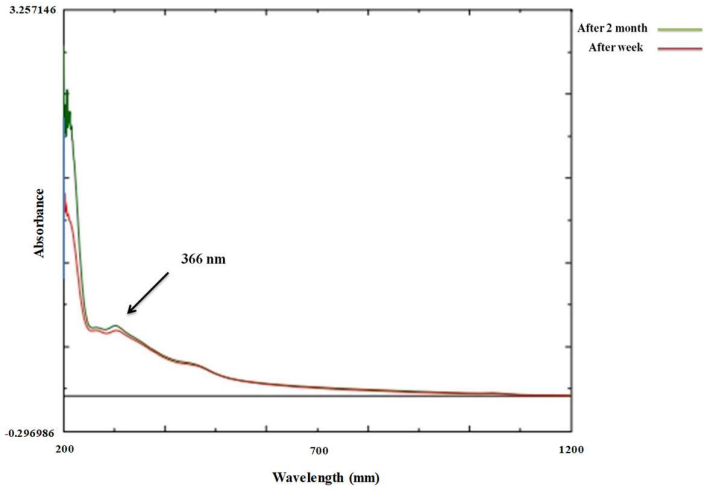

Figure 1 UV-Vis of ZnONPs per.

3.1.2 FTIR spectrum

FTIR spectrum for dried, powdered for (per and m) and ZnONPs (per and m) was obtained in the range of 400-4000 cm^{-1}. The spectra image of FTIR for (per and m) and ZnO NPs (per and m) in the present study is shown in Figure 2,3 Table 1,2. The spectra image of m powder included various peaks of 3417, 2938, 1734, 1617, 1446, 1383, 1351, 1228, 1053, 875, 749 and 621 cm^{-1} Figure 2 (A), Table 2. Whereas The FTIR spectra of per powder contained various peaks of 3407, 2933, 1730, 1617, 1446, 1348, 1228, 1051, 875, 748 and 632 cm^{-1} Figure 2 (B), Table 3.

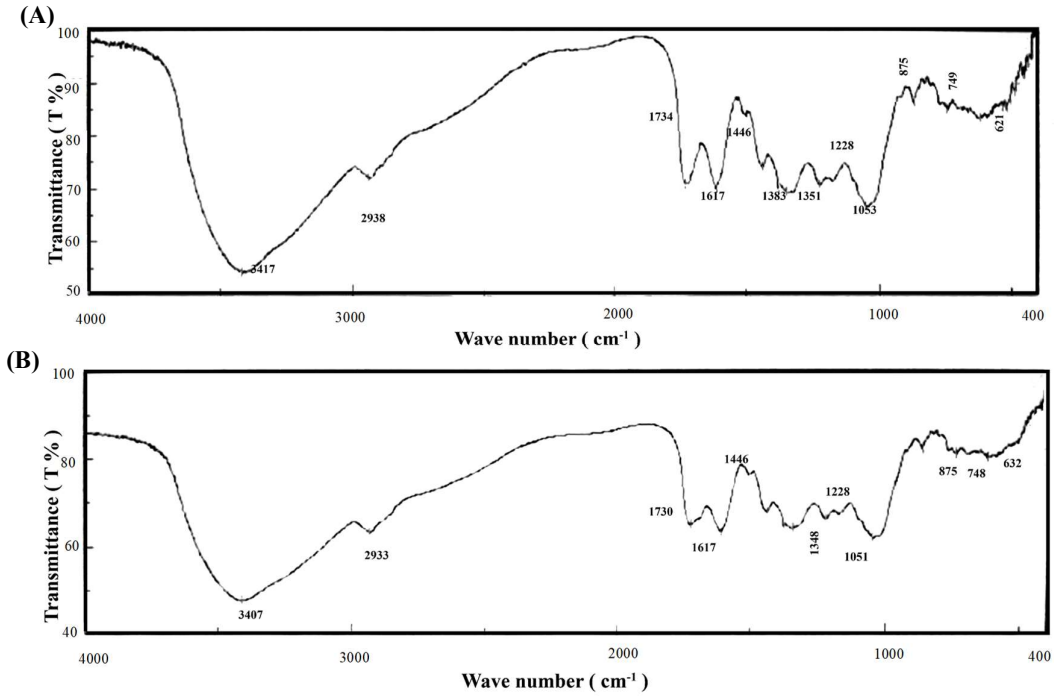

Figure 2 FTIR spectra (A) FTIR of m (B) FTIR of per.

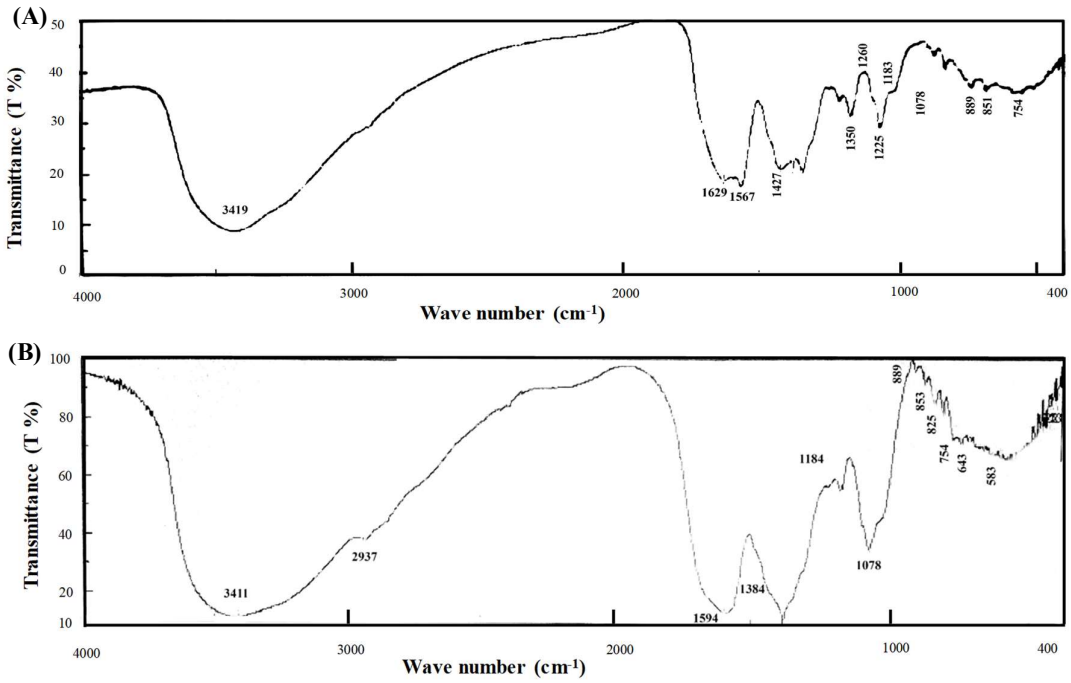

Figure 3 FTIR spectra (A) FTIR of ZnONPs (m) (B) FTIR of ZnONPs (per).

The FTIR spectra of ZnONPs m showed various peaks of 3419, 1629, 1567, 1427, 1384, 1350, 1260, 1225, 1183, 1078, 889,851, 754, 700 and 571 cm^{-1} Figure 3 (A), Table 2. The FTIR spectra of ZnONPs per showed various peaks of 3411, 2937, 1594, 1384, 1184, 1078, 889, 853, 825, 754, 643 and 583 cm^{-1} Figure 3 (B), Table 3.

Table 2 Functional groups of membrane (m) before and after synthesis of ZnONPs.

FTIR of ZnONPs (m)	Functional group	FTIR of membrane	Functional group
3419	O-H stretch, H-bonded Poly Hydroxy compound	3417	O-H stretch, H-bonded Poly Hydroxy compound
-	-	2938	O-H stretch bond of carboxylic acid functional groups, and the -C-H stretch of alkanes
-	-	1734	Ester
1629	Amide, Alkenyl C=C stretch	1617	C=O stretching vibration, Ketone group Ketone compound
1567	Secondary amine, >N-H bend	-	-
1427	stretching of C-C in the aromatic groups	1446	aromatic groups
1384	O-H bending phenol	1383	O-H bending phenol
1350	C-N stretch of the aromatic amines and the carboxylic acid	1351	C-N stretch of the aromatic amines and the carboxylic acid
1260	Primary or secondary, OH in-plane bend (Alcohol and hydroxy compound)	-	-
1225	Aryl-substituted C=C (alkene)	1228	Aryl-substituted C=C (alkene)
1183	C-N stretch (aliphatic amines)	-	
1078	C-H alkenes	1053	C-N stretch of aliphatic amines
889	Vinylidene C-H out-of-plane bend (alkene)	875	Aliphatic chloro compounds, C-Cl stretch
851	P-O-C stretch Aromatic phosphates		-
			Aliphatic chloro compounds, C-Cl stretch
754	Aromatic	749	
700	Aliphatic chloro compounds, C-Cl stretch		-
-	-	621	Alkyne C-H bend
571	Disulfides (C-S stretch) Thiols and thio-substituted compounds		

Table 3 Functional groups of pericarps (per) before and after synthesis of ZnONPs.

FTIR of ZnONPs (per)	Functional group	FTIR of pericarp	Functional group
3411	O-H stretch, H-bonded Poly Hydroxy compound	3407	O-H stretch, H-bonded Poly Hydroxy compound
2937	O-H stretch bond of carboxylic acid functional groups, and the -C-H stretch of alkanes	2933	O-H stretch bond of carboxylic acid functional groups, and the -C-H stretch of alkanes
-	-	1730	Ester
-	-	1617	C=O stretching vibration, Ketone group Ketone compound
1594	Secondary amine, >N-H bend	-	-
-	-	1446	aromatic groups
1384	O-H bending phenol	1348	O-H bending phenol

Table 3 (continued) Functional groups of pericarps (per) before and after synthesis of ZnONPs.

FTIR of ZnONPs (per)	Functional group	FTIR of pericarp	Functional group
-	-	1228	Aryl-substituted C=C (alkene)
1184	C-N stretch (aliphatic amines)	-	-
1078	C-H alkenes	1051	C-N stretch of aliphatic amines
889	Vinylidene C-H out-of-plane bend (alkene)	875	Aliphatic chloro compounds, C-Cl stretch
853	P-O-C stretch Aromatic phosphates	-	-
825	Peroxides, C-O-O- stretch	-	-
754	Aromatic	748	Aliphatic chloro compounds, C-Cl stretch
643	Alkyne C-H bend	632	Alkyne C-H bend
583	Disulfides (C-S stretch) Thiols and thio-substituted compounds	-	-

3.1.3 SEM

SEM images in Figure 4,5 clarify the morphological shape and size of ZnONPs formed from (per and m) respectively. The measurements were taken in six regions for ZnONPs per (36, 36, 30, 45, 25, 28) nm as well as seven regions for ZnONPs m (56, 48, 36, 54, 44, 58, 63) nm with an average diameter of 33-51 nm and spherical shape for both ZnONPs (per and m) Figure 4, 5.

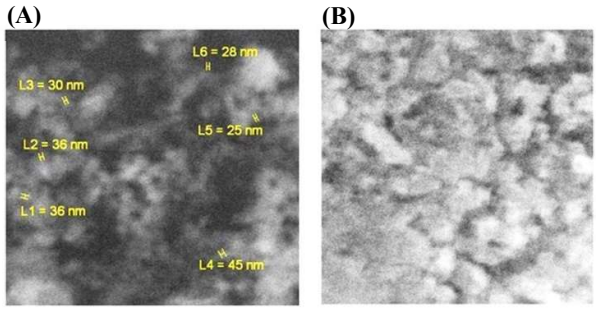

Figure 4 SEM image of ZnONPs (per) spherical shape with (A) (36, 36, 30, 45, 25, 28) nm and (B) 33 nm.

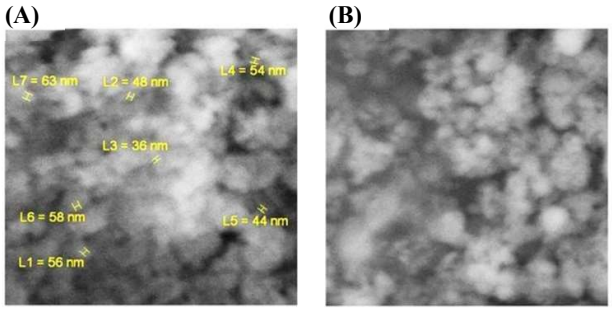

Figure 5 SEM image of ZnONPs (m) spherical shape with (A) (56, 48, 36, 54, 44, 58, 63) nm and (B) 51 nm.

3.1.4 X-ray diffraction (XRD) analysis.

The results of X-ray indicated low crystalline for both NPs with 52 nm average size Figure 6, Table 4.

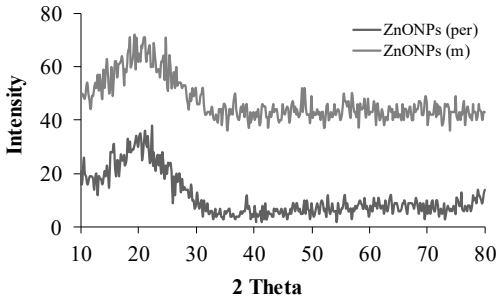

Figure 6 XRD Pattern of ZnONPs (per-m).

Table 4 XRD Pattern of of ZnONPs (per-m).

ZnONPs	Center (2Θ)	FWHM (β)	Center 2	Crystallite size (nm)
m	20.49932	12.03854	37.26402	67
per	20.49932	21.25907	38.74145	37
Average size	52 nm			

3.2 Antibacterial assay

ZnONPs m showed high activity against *S. aureus* strains compared to *E. coli*, the diameter of growth inhibition was 20 mm, while clindamycin had growth inhibition of about 29 mm and 34 mm activity against *S. aureus* for ZnONPs (per and m) respectively. However, the combination of ZnONPs (per and m) solution and clindamycin showed a synergistic effect where the average diameter of inhibition reached 32 and 35 mm respectively, which confirms that the combination of antibiotics such as clindamycin with a solution of ZnONPs (per and m) has a very good effect in the eradication of resistant strains of *S. aureus*. In contrast, ZnONPs (per and m) showed high activity against *E. coli* strains for ZnONPs per compared with ZnONPs m. The average diameter of growth inhibition was 23 and 17 mm respectively, while ciprofloxacin showed high activity against *E. coli*, the average inhibition diameter was 32 and 34 mm for ZnONPs (per and m). However, the best activity appeared against *E. coli* when shared the solution of ZnONPs (per and m) with ciprofloxacin. The average diameter of the inhibition was 37 and 40 mm for ZnONPs (per and m). So, it can be clarified that the strains of *E. coli* are well sensitive to the combination of ciprofloxacin and ZnONPs (per and m) solutions. This could be a result of ZnONPs enhancing ciprofloxacin absorption into the cell [13]. On the other hand, DMSO didn't show any antibacterial effect (Figure 7, Table 5,6).

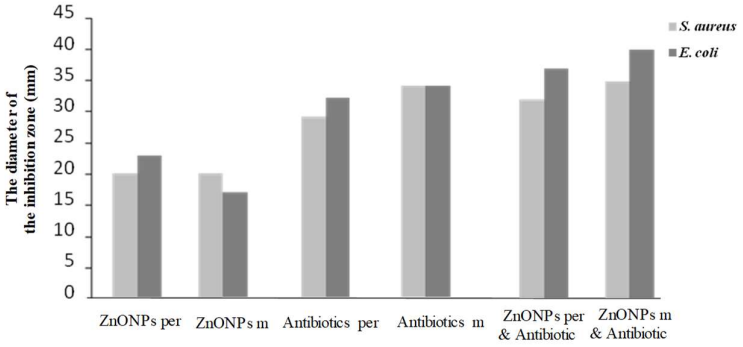

Figure 7 Diagram showing a comparison of inhibition zones for bacterial strains when using ZnONPs per, ZnONPs m, Combination per for (ZnONPs per & Antibiotic) and Combination m for (ZnONPs m & Antibiotic).

Table 5 Antimicrobial activity of synthesized ZnONPs using pericarp (per) of *Punica granatum* extract.

Tested bacteria	ZnONPs per (33 nm)	Antibiotic	Combination of (ZnONPs per & Antibiotic)	DMSO
S. aureus	20	29	32	0
E. coli	23	32	37	0

Table 6 Antimicrobial activity of synthesized ZnONPs using membrane (m) of *Punica granatum* extract.

Tested bacteria	ZnONPs m (51 nm)	Antibiotic	Combination of (ZnONPs m & Antibiotic) m	DMSO
S. aureus	20	34	35	0
E. coli	17	34	40	0

Green Synthesis of ZnO NPs was prepared from pericarp (per) and membrane (m) of pomegranate peel extracts. In this study ZnONPs (per and m) were characterized via changing the color from yellow to white precipitates. The UV-visible spectra illustrated the formation of ZnONPs (per and m) at 366 and 369 nm respectively. A similar study indicated the synthesis of ZnONPs from pomegranate aqueous peel extract where a peak at 369.12 nm was obtained [17]. In contrast other studies reported the UV-Vis spectrum of ZnONPs showed at 300 nm [21], and at broad peaks in the region of 250-480 nm [20]. The difference in absorption peaks is due to the different genotypes of pomegranate and ratios of active substances of secondary metabolites. This also affects the size and shape of the NPs [22]. Our results showed that the size of ZnONPs for (per and m) was 33-51 nm respectively. The SEM images of all ZnONPs confirm the spherical shape. Abdelmigid et al. [21] mentioned that the shape of ZnONPs was hexagonal crystalline with 118.6 nm in size. Also, Husain et al. [17] reported that the morphological shape and size of ZnONPs was crystal shapes with a 42.87 nm. Moreover, Singh et al. [20] indicated SEM images of ZnONPs were nanoplates clusters and 80-100 nm size. Also, our results indicated that in the XRD patterns were amorphous structure. This is agreed with Raad Taher et al. [23] who mentioned that XRD patterns for ZnO NPs were very small and stabilized structure as well as the average size was 53 nm. Likewise, Bagabas et al. [24] and Abdelmigid et al. [21] reported that ZnONPs biologically synthesized appeared in low peak intensity in the XRD spectrum.

The light absorption in the infrared region of most molecules corresponds specifically to the bonds present in it. These bonds appear as peaks in the spectra images due to the presence of different functional groups [17-20-21-25-26-27].

FTIR analysis of *P. granatum* (m) affirmed the presence of functional groups such as poly hydroxy compounds, carboxylic acid, alkanes, ester, ketone, phenol, aromatic amines, aliphatic amines, aliphatic chloro compounds, alkyne, and alkene. Likewise, the same compounds are present in spectra images for *P. granatum* (per) except for the absence of aromatic amines.

Whereas, after the ZnONPs synthesizing, the functional groups change due to their contribution to reducing, stabilizing, and capping NPs. The section among 500 and 890 cm^{-1} is related to ZnONPs in FTIR of *P. granatum* (m and per) [28-30].

Our results of FTIR ZnONPs m indicated transmissions in the vibration band of the ketone compound from 1617 cm^{-1} to a high wavelength of 1629 cm^{-1} (amide) and from 1446 cm^{-1} to a lower wavelength of 1427 cm^{-1} (the aromatic groups) as well as from aliphatic amines at 1053 cm^{-1} to a high wavelength of alkenes (1078) cm^{-1}. Likewise aliphatic chloro compounds at (875-749) cm^{-1} transmit to a high wavelength of (889-754) cm^{-1} (alkene and aromatic).

The absence of bio compounds such as carboxylic acid, alkanes, ester, and alkyne in the spectrum for synthesized ZnONPs (m). Also, peaks appear at (1567, 1260, 1183, 851 and 700) cm^{-1} for secondary amine, alcohol, and hydroxy compound, (aliphatic amines), aromatic phosphates and aliphatic chloro compounds respectively, indicate its contribution to NPs formation.

While our results of FTIR ZnONPs per presented changes in the vibration band of the phenol compound from 1348 cm^{-1} to a high wavelength of 1384 cm^{-1} and from 1051 cm^{-1} (aliphatic amines) to a high wavelength of 1078 cm^{-1} (alkenes) as well as aliphatic chloro compounds at (875-748) cm^{-1} transmit to a high wavelength of (889-754) cm^{-1} (alkene and aromatic). Likewise, the vibration band of the alkyne changed from 632 cm^{-1} to a high wavelength of 643 cm^{-1}.

The absence of functional groups such as ester, ketone, aromatic groups, and alkene in the spectrum for synthesized ZnONPs (per) in addition, peaks appear at (1554, 1184, 853, 825 and 583) cm^{-1} for secondary amine, aliphatic amines, aromatic phosphates, and peroxides respectively, produce by its contribution to the formation of NPs.

The antibacterial activity of ZnONPs per-m solution was evaluated and compared with antibiotic ciprofloxacin and clindamycin which are known for their tested antibacterial activity for *E. coli* and *S. aureus* respectively in Figure 5.

Fontecha-Umaña et al. [31] indicated that the size of inhibition zone was related to the type of bacteria, the concentrations of ZnONPs and its size. So, they mentioned that 10 mg/mL of ZnONPs which inhibited the growth of bacteria was 19 mm for *E. coli* and 29 mm for *S. aureus*.

Our results agree with other reports about that the susceptibility of gram-positive bacteria to ZnONPs could be related to differences in the structure of cell wall, metabolism, and cell physiology [20-30-31]. In addition, the effect varies with the size of NPs, the ZnONPs per were smaller-sized at about 33 nm compared with ZnONPs m at about 51 nm and exhibited better inhibition activities against *E. coli*, this is in agreement with Sukri et al. [7]. Likewise, singh et al. [20] mentioned that ZnONPs per with (80-100 nm, 0.1-1 mg/mL) inhibited *E. coli* growth. On the contrary, Abdelmigid et al. [21] showed that ZnONPs_PPE with (118.6 nm, 2, 4, 8 mg/mL) didn't have any antibacterial activity.

Recent studies explain the mechanism of increased activity of ciprofloxacin in synergy with ZnONPs via many points: a) Increased absorption of ciprofloxacin into the cell via Interference of ZnONPs with NorA protein and membrane Omf protein. b) The structure of ciprofloxacin molecule which has 3 amino groups, fluore group and carboxyl group contributes to strong interaction with ZnONPs. In addition, the action mechanism of ZnONPs can be explained as penetration of the bacterial cell wall inducing oxidative stress, where Zn^{+} ion interacts with the bacterial thiol respiratory enzyme group causing bacterial cell damage [31]. Also, the accumulation of ZnONPs in the cytoplasm and then interaction with biomolecules leads to cell apoptosis and cell death at the end [30].

4. Conclusion

ZnONPs (per and m) can be biologically prepared using aqueous extracts of pomegranate peels. There were many bio-compounds responsible for the conversion into ZnONPs as reducing and capping agents such as ketones, alkenes, and phenols. ZnONPs were characterized by using UV-Vis, FTIR, SEM and X-ray diffraction XRD. ZnONPs are considered a promising inorganic material that has suitable properties to act as an antibacterial active on both gram-positive and gram-negative bacteria. Also, ZnONPs had a good synergy when combined with antibiotics. The effectiveness of NPs depends on several aspects such as NPs shape, size, concentration, and plant genotype. Wherefore, the mechanism of NPs effect needs further research.

5. Acknowledgments

The authors are grateful to Al-Baath University and medico for supporting this research.

6. References

[1] Ahmad S, Munir S, Zeb N, Khan B, Ullah A, Ali J, et al. Green nanotechnology: a review on green synthesis of silver nanoparticles-an ecofriendly approach. Inter J Nanomedicine. 2019;14:5087-5107.

[2] Dhand C, Dwivedi N, Jun Loh X, Jie Ying AN, Verma NK, Beuerman RW, et al. Methods and strategies for the synthesis of diverse nanoparticles and their applications: a comprehensive overview. RSC Adv 5. 2015;127:105003-105037.

[3] Thunugunta T, Reddy AC Reddy LDC. Green synthesis of nanoparticles: current prospectus. Nanotechnol Rev. 2015;4(4):303-323.

[4] Alnaddaf LM, Almuhammady AK, Salem KFM, Alloosh MT, Saleh MM, AI-Khayri JM. Green synthesis of nanoparticles using different plant extracts and their characterizations. In: AI-Khayri J, Ansari MI, Singh AK, editors. Nanobiotechnology. Cham: Springer; 2021. p. 165-199.

[5] Gupta M, Tomar RS, Mishra RK. Factors affecting biosynthesis of green nanoparticles. Our Heritage. 2020;68:10535-10555.

[6] Fuku X, Diallo A, Maaza M. Nanoscaled electrocatalytic optically modulated ZnO nanoparticles through green process of *Punica granatum* L. And their antibacterial activities. Int J Electrochem. 2016;1:1-10.

[7] Sukri SNAM, Shameli K, Wong MM, et al. Cytotoxicity and antibacterial activities of plant-mediated synthesized zinc oxide (ZnO) nanoparticles using *Punica granatum* (pomegranate) fruit peels extract. J Mol St. 2019;1189:57.

[8] Singh B, Singh JP, Kaur A, Singh N. Phenolic compounds as beneficial phytochemicals in pomegranate (*Punica granatum* L.) peel: A review. Food Chem. 2018;261:75-86.

[9] Ifeanyichukwu UL, Fayemi O E, Ateba CN. Green synthesis of zinc oxide nanoparticles from pomegranate (*Punica granatum*) extracts and characterization of their antibacterial activity. Molecules. 2020;25(19):4521.

[10] Siddiqi KS, Tajuddin AUR. Husen A. Properties of zinc oxide nanoparticles and their activity against microbes. Nanoscale Res Lett. 2018;13:141

[11] Chaudhry Q, Scotter M, Blackburn J, Ross B, Boxall A, Castle L, et al. Applications and implications of nanotechnologies for the food sector. Food Add Cont: Part A 25. 2008;25(3):241-258.

[12] Abebe B, Zereffa EA, Tadesse A, Murthy HCA. A Review on enhancing the antibacterial activity of ZnO: mechanisms and microscopic investigation. Nanoscale Res Lett. 2020;15:190.

[13] Allahverdiyev AM, Kon KV, Abamor ES, et al. Coping with antibiotic resistance: combining nanoparticles with antibiotics and other antimicrobial agents. Expert Rev Anti Infect Ther. 2011;9(11):1035-1052.

[14] Ahmad T, Khaddam W, Alnaddaf L, Alloosh M. *Aspergillus niger* as a bio-lab for extracellular synthesis of silver nanoparticles and its antibacterial activity. Bull Pharm Sci. 2022;45(1):427-436.

[15] Thati V, Roy AS, Ambika Prasad MVN, Shivannavar CT, Gaddad SM. Nanostructured zinc oxide enhances the activity of antibiotics against *Staphylococcus aureus*. J Biosci Tech. 2010;1(2):64–69.

[16] Banoee M, Seif S, Nazari Z, Jafari-Fesharaki P, Shahverdi HR, Moballegh A, et al. ZnO nanoparticles enhanced antibacterial activity of ciprofloxacin against *Staphylococcus aureus* and *Escherichia coli*. J Biomed Mater Res B Appl Biomater. 2010;93(2): 557-561.

[17] Husain WM, Araak JK, Ibrahim OMS. Green synthesis of zinc oxide nanoparticles from (*Punica granatum* L.) pomegranate aqueous peel extract. The Iraqi J Vet Med. 2019;43-52.

[18] Santhoshkumar J, Kumar SV, Rajeshkumar S. Synthesis of zinc oxide nanoparticles using plant leaf extract against urinary tract infection pathogen. Resour Technol. 2017;3(4):459-465.

[19] Arrack JK, Hussen WM. Protective role of pomegranate peel extract on testis in adult male rabbits treated with carbon tetrachloride. Iraqi J Vet Med. 2014;38(1):74-82.

[20] Singh M, Lee KE, Vinayagam R, Kang SG. Antioxidant and antibacterial profiling of pomegranate-pericarp extract functionalized-zinc oxide nanocomposite. B. B. E. 2021;1-10.

[21] Abdelmigid HM, Hussien NA, Alyamani AA, Morsi MM, AlSufyani NM, kadi HA. Green synthesis of zinc oxide nanoparticles using pomegranate fruit peel and solid coffee grounds vs. chemical method of synthesis, with their biocompatibility and antibacterial properties investigation. Molecules. 2022;27: 1236.

[22] Sultana F, Barman J, Kalita M. Biogenic synthesis of zno nanoparticles using *Polygonum Chinense* leaf extract and their antibacterial activity. Int J Nanotechnol Appl. 2017;11(2):155-165.

[23] Raad Taher M, Al-Kifaie MAA. Fabrication of Zn/ZnO Core/Shell Nanoparticles by Laser Ablation in Liquid Technique. JK-Physics. 2022;14:32-40.

[24] Bagabas A, Alshammari A, Aboud MF, Kosslick H. Room-temperature synthesis of zinc oxide nanoparticles in different media and their application in cyanide photodegradation. Nanoscale Res Lett. 2013;8:516.

[25] Fazlzadeh M, Khosravi R, Zarei A. Green synthesis of zinc oxide nanoparticles using *Peganum Harmala* seed extract, and loaded on *Peganum Harmala* seed powdered activated carbon as new adsorbent for removal of Cr (VI) from aqueous solution. Ecol Eng. 2017;103:180-190.

[26] Ishwarya R, Vaseeharan B, Kalyani S, Banumathi B. Facile green synthesis of zinc oxide nanoparticles using *Ulva Lactuca* seaweed extract and evaluation of their photocatalytic, antibiofilm and insecticidal activity. J Photochem Photobiol Biol. 2018;178:249-258.

[27] Ghidan AY, Al-Antary TM, Salem NM, Awwad AM. Facile green synthetic route to the zinc oxide (ZnONPs) nanoparticles: Effect on green peach aphid and antibacterial activity. J Agric Sci. 2017;9(2): 131.

[28] Nava OJ, Luque PA, Gómez-Gutiérrez CM, Vilchis-Nestor AR. Influence of Camellia sinensis extract on Zinc Oxide nanoparticle green synthesis. J Mol Struct. 2017;1134:121-125.

[29] Sharif M, Ansari F, Malik A, Ali Q. Fourier-Transform Infrared Spectroscopy, antioxidant, phytochemical and antibacterial screening of nhexane extracts of *Punica granatum*, A Medicinal Plant. GMR. 2020;19(4):gmr16039989.

[30] Emami-Karvani Z, Chehrazi P. Antibacterial activity of ZnO nanoparticle on gram positive and gram-negative bacteria. Afr J Microbiol Res. 2011;1368-1373.

[31] Fontecha-Umaña F, Ríos-Castillo A, Ripolles-Avila C, Rodríguez-Jerez J. Antimicrobial activity and prevention of bacterial biofilm formation of silver and zinc oxide nanoparticle-containing polyester surfaces at various concentrations for use. Foods. 2020;9:4.